Pedosphere ISSN 1002-0160/CN 32-1315/P doi:10.1016/S1002-0160(21)60048-6

Inhibiting ammonia-oxidizing bacteria promotes the growth of ammonia-oxidizing archaea in ammonium-rich alkaline soils

Chinese title: 抑制氨氧化细菌促进高氮碱性土壤中氨氧化古菌的生长

Running title: Inhibiting AOA promotes AOB growth

Chang YIN[1], Xiaoping FAN[1], Hao CHEN[1], Mujun YE[1], Guochao YAN[1], Tingqiang LI[1], Hongyun PENG[1], Shengzhe E[2], Zongxian CHE[2], Steven A. WAKELIN[3] and Yongchao LIANG[1,*]

[1]*Key Laboratory of Environment Remediation and Ecological Health, Ministry of Education, College of Environmental &Resource Sciences, Zhejiang University, Hangzhou 310058 (China)*
[2]*Institute of Soil and Fertilizer and Water-Saving Agriculture, Gansu Academy of Agricultural Sciences, Lanzhou 730070 (China)*
[3]*Scion Research, PO Box 29237, Christchurch 8011 (New Zealand)*

Highlights

1. Inhibiting AOB promotes the growth of taxonomically constrained AOA
2. Some AOA phylotypes occupy broader niches than previously believed
3. DMPP specifically inhibited AOB in the alkaline soils tested

ABSTRACT

The disparities in substrate affinity and tolerance threshold for ammonia have been believed to play a key role in driving niche differentiation between ammonia-oxidizing archaea (AOA) and bacteria (AOB), while recent surveys argue that direct competition between them is of importance in this phenomenon as well. Accordingly, it is reasonable to predict that diverse AOA lineages would grow in ammonium-rich alkaline arable soils if AOB growth was suppressed. To test this hypothesis, a microcosm study using three different types of alkaline arable soils was established in which high ammonium concentration (200 μg N g^{-1} dry soil) was maintained by routinely replenishing urea, and activities of AOB were selectively inhibited by 1-octyne or 3, 4-dimethylpyrazole phosphate (DMPP). The results indicated that compared with sole amendment with urea, 1-octyne treatment partially retarded the growth of AOB while DMPP completely inhibited AOB; both inhibitors accelerated the growth of AOA, with significantly higher ratios of abundance of AOA to AOB being observed in

*Corresponding author. E-mail: ycliang@zju.edu.cn.

DMPP amendments across soils. Non-metric multidimensional scaling analysis (NMDS) indicated that different treatments significantly altered the community structures of both AOA and AOB, and AOA OTUs enriched by high-ammonium amendment were taxonomically constrained across the soils tested and closely related to *Nitrososphaera viennensis* EN76 and *N. garnensis*. Given that these representative strains have been demonstrated to be sensitive to high ammonia concentrations adopted here, our results thus suggest that it is the competitiveness for ammonia rather than disparities in substrate affinity and tolerance threshold for ammonia that drives niche differentiation between these phylotypes and AOB in ammonium-rich alkaline soils.

Key Words: AOA; niche differentiation; ammonia; 1-octyne; DMPP

INTRODUCTION

Ammonia oxidization, the key component and rate-limiting step of aerobic nitrogen cycling, had been thought to be primarily conducted by certain lineages of *Beta-* and *Gamma-proteobacteria* for more than a century (Koops and Pommerening-Röser, 2001). However, the discovery of AOA has fundamentally changed our understanding of the biogeochemistry of nitrogen cycling in aquatic and terrestrial environments (Francis *et al.*, 2005; Leininger *et al.*, 2006). In many ecosystems, AOA are numerically more abundant than AOB; this leads to the speculation that AOA assume a functionally-significant role in nitrification and, consequently, regulation of the ecosystem N-cycling (Francis *et al.*, 2005; Leininger *et al.*, 2006).

In soils, AOB typically prevail in NH_4^+-rich conditions while AOA dominate environments with low NH_4^+ concentrations (Hatzenpichler, 2012; He *et al.*, 2012; Prosser and Nicol, 2012). These niche-associated differences, linking to AOA and AOB numerical and functional dominance, have been frequently invoked to explain the variation in nitrification activity among soil ecosystems (Hatzenpichler, 2012; He *et al.*, 2012; Prosser and Nicol, 2012), and demonstrated to have a profound mechanistic basis, as cultivated AOA and AOB show substantial disparities in physiological traits (Martens-Habbena *et al.*, 2009; Prosser and Nicol, 2012; Stahl and de la Torre, 2012). Importantly, most cultivated AOA strains have a higher affinity for NH_3/NH_4^+ (*i.e.*, K_m value) than AOB (Martens-Habbena *et al.*, 2009; Hatzenpichler, 2012; Prosser and Nicol, 2012; Kits *et al.*, 2017), and this has been proposed as a key mechanism by which AOA dominate nitrification activity in oligotrophic environments including acidic soils where the availability of substrate, NH_3, is exponentially decreased due to the ionization (Lehtovirta-Morley *et al.*, 2011; He *et al.*, 2012). On the other hand**,** their higher sensitivity to NH_3/NH_4^+ has been believed to restrict growth under high NH_3/NH_4^+ concentrations (Verhamme *et al.*, 2011; He *et al.*, 2012; Prosser and Nicol, 2012), such that AOB dominate nitrification in NH_4^+-rich neutral-alkaline soils (Di *et al.*, 2009; Verhamme *et al.*, 2011; Xia *et al.*, 2011).

While these physiological disparities between AOA and AOB provide compelling explanations for their varying activities in different environments, such prevailing paradigms have recently been questioned. Emerging physiological analyses failed to support that there are meaningful differences in the NH_3 affinity between several typical AOA and AOB strains (Hink *et al.*, 2017; Kits *et al.*, 2017). And, isolates of the *Nitrosocosmicus* lineage that grow in NH_3 concentration as high as 1.49 mM,

similar to that of copiotrophic AOB, have been documented (Jung *et al.*, 2016; Lehtovirta-Morley *et al.*, 2016; Sauder *et al.*, 2017). Therefore, it is likely that a few, at least some, AOA phylotypes potentially adapt to growth in NH_3-rich neutral-alkaline soils. This notion is supported by studies reporting that multiple phylotypes within *Nitrosopumilales* and *Nitrososphaerales* lineages grew moderately in soils that were continually amended with a high amount of NH_4^+ (Verhamme *et al.*, 2011; Alves *et al.*, 2018), and further strengthened by recent research reporting that AOA growth was accelerated under ammonium-rich conditions when the growth of AOB was selectively repressed by inhibitors, 1-octyne or DMPP (Hink *et al.*, 2018; Fan *et al.*, 2019). These studies point out that niche differentiation between AOA and AOB might stem not only from their differences in ammonia oxidization dynamics but also from direct inter-group competition for the substrate (Hink *et al.*, 2018; Zhao *et al.*, 2020). As such, it is reasonable to hypothesize that release from competition with AOB may support the growth of AOA in NH_4^+-rich alkaline soils; and if present, this phenomenon may not be soil specific or restricted to a narrow range of AOA lineages.

Therefore, the main objective of this study was to explore the possibility that diverse AOA lineages could thrive in high NH_4^+ alkaline arable soils ($7.7 < pH < 8.4$). To achieve this, three soils differing in basic physicochemical properties (*e.g.*, pH, organic matter content, available potassium, and nitrate etc.) were collected from different regions of China, a microcosm experiment was then established, in which a high concentration of NH_4^+ (*i.e.*, 200 μg g^{-1} N dry weight soil) was maintained by routinely amending with urea and the growth of AOB was selectively inhibited by 1-octyne (Taylor *et al.*, 2013). In comparison, DMPP was further selected to retard the growth of AOB based on earlier findings (Shi *et al.*, 2016; Fan *et al.*, 2019). Taking advantage of multiple molecular ecological tools, we focused on testing the hypothesis that diverse AOA lineages, in particular those of *Nitrosocosmicus* lineage, would prevail in NH_4^+-rich alkaline arable soils if the growth of AOB was suppressed.

MATERIALS AND MATHODS

Soil sampling and determination of soil properties

Three alkaline arable soils (*i.e.*, Luoyang, Shihezi, and Tianshui), all previously characterized as being AOB-dominated with regard to nitrification activity (Xia *et al*., 2011; Tao *et al*., 2017; Yin *et al*., 2017), were used in this study. The fluvo-aquic soil was collected from Luoyang City, Henan Province, the grey desert soil from Shihezi City, Xinjiang Uyghur autonomous region, and the loessial soil from the Zhongliang long-term fertilization experiment station, Tianshui City, Gansu Province (see Table I for georeferencing). These sites, spanning a wide geographic range, differed greatly in meteorological and physio-chemical properties, as well as management practices (Table I). Bulk soil (0--20 cm) was collected at each site, sieved through a 2-mm mesh, and stored at 4 °C. The detailed sampling design and determination of basic soil properties were presented in supplemental materials.

TABLE I

Meteorological parameters of sampling sites and basic physicochemical properties of soils

Item	Luoyang	Shihezi	Tianshui

Location	34°27′ N, 113°01′ E	44°23′ N, 85°41′ E	34°36′ N, 105°38′ E
Soil type	Fluvo-aquic soil	Grey desert soil	Loessial soil
Cultivated crops	Wheat/maize	Grape	Wheat/canola
MAP (mm)	620	225	491
MAT (°C)	15	7.8	11
Annual range of temperature (°C)	-3–32	-17--32	-6--30
pH (H_2O)	7.80	8.35	7.66
TN (g kg^{-1})	1.12	0.96	1.03
OM (g kg^{-1})	19.03	13.27	14.78
TP (g kg^{-1})	0.827	0.861	0.898
Available K (mg kg^{-1})	199.85	98.48	140.03

Microcosm experiment

The 27-d microcosm incubation experiment with five treatments for each of the three soil types was established. These treatments included no fertilizer control ('CK'), the addition of urea ('Urea'), the addition of urea with 10 Pa C_2H_2 ('Urea+C_2H_2'), the addition of urea with 1-octyne (C_{aq} = 4 μM; 'Urea+1-Octyne'), and addition of urea with DMPP (1.5% of added urea N; 'Urea+DMPP'). The C_2H_2 treatment was used to inhibit all autotrophic nitrification activity, while 1-octyne and DMPP are considered to have specificity to inhibition of AOB growth (Taylor *et al.*, 2013; Fan *et al.*, 2019). All soils were pre-incubated at 25 °C for 15 d at 30% water holding capacity (WHC). Microcosms were established by weighing pre-incubated soil (15 g dry wt. equivalent) into 125 ml serum bottles sealed with butyl stoppers and aluminum caps. In each microcosm, the soil moisture was adjusted to 50% WHC with deionized water, urea, C_2H_2, 1-octyne, or DMPP according to treatment design. Thirty microcosms were established for each treatment. For treatments other than CK, urea was initially added at a rate of 200 μg NH_4^+-N g^{-1} dry soil and maintained by regularly replenishing throughout incubation at an interval of 6 days. Varying amounts of urea were replenished on the basis of measured NH_4^+ concentration to maintain the concentration of 200 μg NH_4^+-N g^{-1} dry soil during the incubation. For instance, in Luoyang soil, the concentration of NH_4^+-N in the Urea treatment was 2.29 μg g^{-1} at day 6, 197.71 μg Urea-N g^{-1} was supplemented into the corresponding microcosms; while that of Urea+DMPP was 119.16 μg g^{-1}, 80.84 μg Urea-N g^{-1} was then replenished. The CK treatment was added with an equivalent volume of water only.

At the end of the incubation, the soil moisture of all treatments reached 60% WHC. All microcosms were incubated at 25 °C. Following microcosm setup, 2 h was allowed for solutions to adequately diffuse in soils and the first batch of samples was collected; these are designated as 'day 0'. Three bottles per treatment were randomly selected at an interval of 3 d for the determination of NH_4^+ and NO_3^-. Samples collected on days 0, 3, 9, 15, 21, and 27 were used for molecular ecological analysis as well as the determination of pH values. All samples were stored at -80 °C until use. All microcosms were regularly ventilated for 30 min every 3 d; C_2H_2 and 1-octyne were refreshed in the headspace of their respective treatment flasks.

T-RFLP analysis and Quantitative PCR (q-PCR)

DNA was extracted from 500 mg of soil using Fast DNA SPIN Kit for soil with a FastPrep-24 machine (Qbiogene, Canada). Terminal restriction fragment length polymorphism (T-RFLP) analysis of bacterial and archaeal *amoA* genes was determined over the CK sample on day 0, and all treatment samples at days 15 and 27. The PCR amplification conditions were presented in Table S1 and raw data analysis procedures have been reported previously (Yin *et al.*, 2017). Bacterial and archaeal *amoA* genes were quantified in DNA samples from days 0, 3, 9, 15, 21, and 27. The qPCR reactions were carried out in triplicate per experimental sample on a LightCycler® 480II (Roche Diagnostics, Switzerland) using SYBR green chemistry. Primer pairs and thermal cycling conditions for amplification were supplied in Table S3. Each 15 μL PCR mixture contained 0.3 μM each primer, 7.5 μL of TSINGKEMasterqPCR mix (Qingke, China), and 2 μL of 20-fold diluted DNA. Standard curves for real-time PCR (qPCR) were constructed by 10-serial dilution of known copy number plasmids harboring the gene of interest. Three replicates of no-template negative control were included and gave negligible values. The R^2 were > 0.996 for both genes and the amplification efficiency was 82% for AOA, and 93% for AOB, respectively.

Amplicon sequencing of AOA and AOB amoA genes

At the end of the incubation (day 27), high throughput sequencing of AOA and AOB *amoA* genes was conducted using the Illumina MiSeq sequencing platform (PE300 chemistry). For AOB, barcoded amoA1F/amoA2R primers were used. The barcoded Arch-amoAF/Arch-amoAR primer pairs were used for AOA. PCR conditions for both genes were presented in Table S3. To accommodate the requirement for analysis of AOA *amoA* gene (> 600 bp for total length), only forward single-end sequences were analyzed in this study. Briefly, raw sequences for both genes were firstly quality screened using "fastp" (Chen *et al*., 2018) keeping sequences of > 50 bp with an average Phred score of > 20. Then, the pair-ended reads for bacterial *amoA* gene were merged using FLASH (version1.2.11) (Chen *et al*., 2018) with minimum overlap of 10 bp. Both AOA and merged AOB *amoA* sequences were further de-replicated with "vsearch" (Rognes *et al*., 2016). Thereafter, chimeric sequences were filtered away with UCHIME (Edgar *et al*., 2011); resulting valid sequences were clustered into operational taxonomic units (OTUs) at 97% similarity using Uparse (Edgar, 2013). All these analysis were conducted on the integrated Majorbio Cloud Platform (www.Majorbio.com). Representative OTUs of AOA and AOB were further validated by BLAST against the NCBI nucleotide database, followed by translation to amino acids and alignment with the database curated by others (Alves *et al.*, 2018; Jones and Hallin, 2019) in MEGA 6.0 (Tamura *et al.*, 2013). The final classification was based on the taxomony proposed by Alves *et al*. (2018) and Jones and Hallin (2019). All raw *amoA* gene sequence data is available at NCBI under the accession number PRJNA579399.

Statistical analysis

The phylogenetic analysis of AOA and AOB was conducted in MEGA 6.0 (Tamura *et al.*, 2013) and visualized using iTOL (http://itol.embl.de) (Letunic and Bork, 2016)). Statistical analysis was conducted in R. 3.6.1 (R Core team, 2019). One-way ANOVA was used to assess the temporal changes in pH, NH_4^+, and NO_3^- concentrations, as well as the abundances of AOA and AOB among soil types. Variation in treatment means was assessed using Tukey's *post hoc* test. Differences in

relative abundances of OTUs among treatments were assessed with the Kruskal-Wallis rank test at α = 0.05. Variation in the presence of *amoA* OTUs (AOA and AOB) in soils was conducted in the '*vegan*' package (Oksanen *et al.*, 2019). Principal component analysis (PCA) was used to explore the temporal shift in the occurrence of AOA and AOB genes across treatments and soils. Permutational analysis of variance (PERMANOVA) was used to test the effect size and significance of treatments, and these were visually interpreted using non-metric multidimensional scaling (NMDS).

RESULTS

The changes in ammonium, nitrate, and pH

The dynamics of soil ammonium and nitrate concentration, as well as pH, were monitored over the incubation. Around 30-50% of added urea was hydrolyzed to ammonium within the initial 2 hours stabilization period in urea-amended treatments (Fig. 1), and complete hydrolysis was achieved within 12 hours for all three soils tested (data not shown). The NH_4^+ concentrations of no amendment control (CK) approached the analytical detection limit throughout the whole incubation period for all soils, and a detectable buildup of NO_3^- concentration in this treatment was only observed in the soil from Shihezi (one-way ANOVA; $P < 0.001$; Fig. 1e). The NH_4^+concentrations in the C_2H_2 treatments exhibited minor temporal variation, but no significant accumulation of NO_3^- was observed at the end of incubation across all soils (Tukey HSD test; $P > 0.05$). In contrast, NH_4^+ in the urea-only treatment (Urea) was rapidly nitrified into NO_3^- and replenished urea completely converted within 72 h after day 12, leading to a decline of 0.6, 1.0, and 0.5 units in pH for the Luoyang, Shihezi, and Tianshui soils, respectively, relative to their value of CK at the end of incubation (Fig. S1). These findings indicated the occurrence of strong autotrophic nitrification activity for all soils tested. Amendment with DMPP strongly decreased oxidation of NH_4^+ to NO_3^-(Fig. 1). Its effect was higher in soils from Shihezi (Fig. 1b) and Tianshui (Fig.1c), resulting in relatively consistent nitrification rates and stable NH_4^+ concentrations during incubation, such that a decline of smaller magnitude in pH was observed in this treatment of Luoyang (0.31, $P < 0.001$) and Shihezi soils (0.22, $P < 0.001$), but a minor increase (0.07 relative to CK) was observed in the Tianshui soil at day 27 ($P < 0.02$) (Fig. S1). In comparison, 1-Octyne treatment was less effective at inhibiting nitrification, particularly in the Luoyang soil (Fig. 1d). In these treatments with 1-octyne, the pH dropped by 0.51, 0.95, and 0.27 units for Luoyang, Shihezi, and Tianshui soils, respectively (Fig. S1).

Fig. 1 The dynamics of ammonium (a, b, and c) and nitrate (d, e, and f) in Luoyang (a, d), Shihezi (b, e) and Tianshui (c, f). Means ± 1SE (n = 3) were shown. Urea was supplemented in all treatments except CK at days 6, 12, 18, and 24 to reach the targeted ammonium concentration (*i.e.*, 200 μg N g^{-1} dry soil), the times at which urea was supplemented were labeled with arrows.

AOA and AOB amoA gene abundances

Across all soils tested, AOA growth was inhibited in the C_2H_2-treated microcosms (*i.e.*, C_2H_2 treatment), but strongly promoted in both Urea+DMPP and Urea+1-Octyne treatments (Fig. 2a--c). The highest AOA growth rates were generally found in the DMPP-treated soils; the exception was the

Tianshui soil in which similar AOA growth was observed in the Urea+DMPP and Urea+1-Octyne treatments after day 15 (Tukey HSD test, $P > 0.05$), while AOA growth was moderately stimulated in the Urea treatment in Luoyang and Tianshui soils (one-way ANOVA, $P < 0.001$). For all soils, the Urea treatment led to the fastest increase in AOB *amoA* gene numbers, but the addition of C_2H_2 and DMPP with urea completely suppressed AOB growth in soils (Fig. 2d--f). In comparison, the inhibitory effect of Urea+1-Ocytne treatment was moderate, especially in the Shihezi soil (Fig. 2e).

Fig. 2 The changes in abundances of AOA (a, b, and c) and AOB (d, e, and f) in Luoyang (a, d), Shihezi (b, e) and Tianshui (c, f) soil during incubation. Means ± 1SE ($n = 3$) were shown.

The varying degrees of AOA and AOB growth led to different temporal changes in the ratio of the abundance of AOA to that of AOB among treatments (Fig. S2). In general, all Urea+DMPP treatments resulted in an exponential increase in this index, while it was declined by the Urea treatment during the initial 9 d, thereafter kept relatively stable until the end of incubation across soils. The ratios of AOA to AOB in Urea+1-Octyne treatments decreased gradually in Shihezi along with incubation (Fig. S2A) but kept relatively stable in the Luoyang soil (Fig. S2B), and an abrupt increase was observed for the Tianshui soil at day 3 followed by a decline until day 15 (Fig. S2C). Meanwhile, a slight increase in this index was only observed for CK of Shihezi (Fig. S2B) and for the Urea+C_2H_2 treatment of Tianshui (Fig. S2C). At the end of incubation, the ratio of AOA to AOB showed a trend of increase following the order of Urea, Urea+1-Octyne, and Urea+DMPP treatments across soils tested, and this index was significantly higher in DMPP treated soils than in the other treatments (Tukey HSD test, $P < 0.001$) (Fig. S2).

Temporal changes in community structures of AOA and AOB

The temporal shift in AOA and AOB community structures was explored by T-RFLP in combination with PCA ordination (Fig. S3, S4). The major two principal axes accounted for > 80% of the overall separation among samples for all soils (Fig. S4). PERMANOVA tests revealed significant effects of sampling time and treatment on both guilds across soils (Table S1). The dominant AOA T-RFs differed among soils (Fig. S3a--c), while community structures of Urea+1-Octyne and Urea+DMPP treatments in each soil increasingly converged by day 27, separating from other treatments (Fig. S4a--c). This was due to the gradual enrichment of nearly identical T-RFs over the incubation across soils (Fig. S3a--c). The major T-RFs contributing to the shift in overall AOB community structure were similar, but their response patterns to treatments varied among the soils (Fig. S3d--f). In PCA plots, the CK, Urea+C_2H_2, and Urea+DMPP treatments clustered together and were distinct from the Urea+1-Octyne and Urea, and the latter two treatments were dissimilar to one another across all soils (Fig. S4d--f).

Phylogenetic composition of AOA and AOB amoA genes

The phylogenetic composition of AOA and AOB ammonia oxidizers were analyzed by high-throughput sequencing of *amoA* genes from samples collected on day 27. Rarefaction curves indicated that the sequencing depth was sufficient to capture the vast majority of the total diversity

present (Fig. S5). After equalizing effort, 407 295 AOA reads clustered into 113 OTUs at 3% distance sequence dissimilarity, with 90 OTUs being found for Luoyang, 91 OTUs for Shihezi, and 76 OTUs for Tianshui, respectively; while 192 150 AOB reads clustered into 78 OTUs (3% sequence dissimilarity), and 56 OTUs were found for Luoyang, 62 for Shihezi, and 48 for Tianshui (Table S2).

All amplified AOA OTUs were classified as *Nitrososphaerales*, and dominant lineages differed among soils (Fig. S6). Specifically, AOA assemblage in the Luoyang soil primarily comprised *Nitrososphaerales*-δ-1.1.2 (54% of relative abundance), α-3.2.1(20%), γ-1.1 (10%), and γ-2.1.1 (13%) lineages. A similar composition was found for Tianshui soil except for a considerable portion (6%) coming from *Nitrososphaerales*-β-1.1 therein. In the Shihezi soil, *Nitrososphaerales*-β-1.1 was dominant (34%); the α-3.2.3 and α-3.2.4 lineages which were rare in Luoyang and Tianshui soils, contributed another 27% to the reads. Notably, OTUs similar to *Nitrosocosmicus* were very rare across all soils.

For AOB taxa, only two OTUs clustered within the *Nitrosomonas* family (Shihezi soil specific), the remaining being *Nitrosospira* (Fig. S7). The dominant lineages of AOB were similar among soils and primarily composed of taxa from cluster 3. Cluster 3a.1 accounted for > 60% of reads across soils, followed by cluster 3a.2 in Luoyang (25% of relative abundance) and Tianshui soils (22%), and cluster 3b (18%) in soil from Shihezi.

Treatment effects on AOA and AOB amoA genotypes

The effects of treatment on compositional changes in AOA and AOB *amoA* OTUs were analyzed by NMDS (Fig. 3) and further visualized with heatmaps (Figs. 4 and S8). A similar resolution for β-diversity analysis of treatment effect was observed between the NMDS ordination and the PCA analysis of T-RFLP data (Table S1, Fig. 3), suggesting negligible bias introduced by adopting different primer pairs for the analysis of AOA guild; and heatmaps revealed strong differences in compositions of *amoA* OTUs among the soils tested.

Fig. 3 NMDS analysis of the community composition of AOA (a-c) and AOB (d-f) for Luoyang (a, d), Shihezi (b, d), and Tianshui (c, f). All OTUs whose relative abundances were significantly changed by treatments were shown as circles (i. e. the colored numbers). Their relative abundances were log-scaled with the diameter of circles, and phylogenetic affiliations were mapped to different colors. NS, *Nitrososphaerales*.

Fig. 4 Composition of AOA OTUs that were significantly different among treatments within soils. The unrooted phylogenetic tree was shown on the left of the heatmap. The cluster analysis result of samples based on the Bray-Curtis dissimilarity matrix was shown above the heatmap. For clarity, only OTUs with relative abundance higher than 0.1% across all samples were shown.

For AOA, the relative abundances of 28, 37, and 18 OTUs significantly differed among treatments for the Luoyang, Shihezi, and Tianshui soils, respectively (Kruskal-Wallis rank test, $P < 0.05$; Fig. S9a), but none of them were in the ε-2.2, γ-2.2.3, or *Nitrosocosmicus* lineages (Figs. S6 and 3). Among these, seven OTUs were shared by all soils, each of which showed a similar response pattern to given treatment (Figs. 4 and S9a). Moreover, the heatmap shows that the major OTUs enriched by Urea+1-Octyne treatment (i.e. OTUs 13, 21, 20, 22, 26, 75, and 77) were also promoted

by both Urea and Urea+DMPP treatments in all soils (Fig. 4). These OTUs phylogenetically belonged to either *Nitrososphaerale* α-3.2.1 or α-3.2.4 lineages, which are related to *Nitrososphaera viennensis* EN76 and *Nitrososphaera* sp. JG1, as well as *Nitrosophaera gargensis* strains with high bootstrap confidence (Fig. S6). However, their close relatives in α-3.2.3 lineage declined in both Urea and Urea+C_2H_2 treatments compared with other treatments, implying diversification of physiology within phylogenetically associated lineages. In contrast, changed OTUs in β-1, δ-1, γ-1.1, and γ-2.1 lineages were generally reduced by Urea+1-Octyne and Urea+DMPP treatments; interestingly, those of γ lineages mostly showed a trend of increase in Urea+C_2H_2 treatment (Fig. 4).

For AOB, the relative abundances of 17 OTUs for Luoyang, 18 OTUs for Shihezi, and 19 OTUs for Tianshui were significantly changed by treatments (Kruskal-Wallis rank test, $P < 0.05$; Fig. S9b). All of them were assigned to *Nitrosospira* clusters 2 or 3 (Figs. 3 and S8). Seven of these treatment-responsive OTUs were shared across all soils, with six associated with *Nitrosospira* cluster 3a.1 and one to cluster 3a.2 (Figs. S7b and S8). The relative abundances of OTUs in cluster 3b were generally reduced by either Urea or Urea+1-Octyne treatment, and OTUs in cluster 3a.2 tended to decline only in the Urea treatment (Fig. S8). In contrast, OTUs enriched by the Urea treatment (in all tested soils) mainly came from *Nitrosospira* cluster 3a.1, 2a, and 2b, and the majority of them were inhibited by both Urea+C_2H_2 and Urea+DMPP treatments. Meanwhile, diverse shift patterns were observed in cluster 3a. 1. For instance, OTUs 26, 47 and 69, all of which were related to *Nitrosospira multiformis*, showed a trend of increase in Urea+1-Octyne treatment across the soils, while OTUs 54 and 80 were inhibited by 1-octyne (Fig. S8).

DISCUSSION

Underlying ammonia oxidization dynamics in cultivated strains of AOA and AOB, alongside biogeochemical data from field and microcosm studies, has established an understanding that AOA are favored under oligotrophic conditions whereas AOB thrive in moderate acid-alkaline soils with elevated concentrations of NH_4^+ (Hatzenpichler, 2012; He *et al.*, 2012; Prosser and Nicol, 2012). Extended from this, it has been proposed that the relative differences in abundance and functional role of AOB *vs.* AOA in various ecosystems are primarily driven by their disparities in metabolic traits including substrate affinity and tolerance threshold for ammonia, as well as preference for a supply rate of NH_3 (Prosser and Nicol, 2012; Hink *et al.*, 2018; Trivedi *et al.*, 2019). Here, by continually supplying urea and selectively inhibiting AOB, we demonstrate that taxonomically constrained AOA, which had been believed to be sensitive to high NH_3 concentration, prevail in copiotrophic alkaline soil conditions. These findings strongly support the notion that the direct competition for the substrate plays a key role in driving niche differentiation between these AOA phylotypes and AOB in NH_4^+-rich alkaline soils. Furthermore, our results revealed the coherence of ecophysiology within the same phylogenetic lineage of *Nitrososphaerales*.

NH_3 rather than NH_4^+ serves as the direct substrate for autotrophic ammonia oxidizers; differences in substrate affinity and tolerance threshold for NH_3 have been proposed as overarching mechanisms driving niche differentiation between AOA and AOB (Hatzenpichler, 2012; He *et al.*, 2012; Prosser and Nicol, 2012). Indeed, the majority of cultivated AOA exhibit a much higher substrate affinity for NH_3 than their bacterial counterpart, which has been postulated to provide them with advantages under oligotrophic conditions (Martens-Habbena *et al.*, 2009; Lehtovirta-Morley *et*

al., 2011; Tourna *et al.*, 2011; Kits *et al.*, 2017). This appeared to be evident in the untreated Shihezi soil where no AOB growth was observed while AOA populations were sustained by scavenging NH_3 released during organic matter mineralization (Offre *et al.*, 2009). However, it would be of little ecological relevance in environments with high NH_3 concentrations (Hink *et al.*, 2018). For instance, the soil NH_4^+ of Urea+1-Octyne treatment fluctuated between 20 and 200 μg g^{-1} soil in the first 15 days, in particular for Shihezi and Tianshui soils in which the lowest NH_4^+-N concentrations were found to be as high as 117 μg g^{-1} soil. According to the ionization equilibrium $NH_4^+ \rightleftharpoons NH_3 + H^+$ (p*K*a = 9.25; *T* = 25 °C), the lowest NH_3 concentrations were estimated to range from 88 to 528 μM. Such concentrations are much higher than K_m values of both AOA and AOB, even exceed the inhibitory concentration for most cultivated AOA (Hatzenpichler, 2012; He *et al.*, 2012; Prosser and Nicol, 2012), whereas both AOA and AOB grow rapidly and simultaneously during this period. Importantly, AOA grew in both Urea+1-Octyne and Urea+DMPP treatments, and their growth coincided with the inhibition of AOB. This echoed the recent findings that alleviation of competition between AOA and AOB by 1-octyne, DMPP, or simvastatin accelerated the growth of either AOA or AOB under copiotrohic conditions (Hink *et al.*, 2018; Fan *et al.*, 2019; Zhao *et al.*, 2020). Therefore, our results provide evidence that low AOA growth in NH_4^+-rich alkaline arable soils likely extends from their poor competitiveness with AOB rather than disparities in physiological characteristics such as substrate affinity and tolerance threshold for NH_3, as well as preference for a supply rate of NH_3.

The growth of AOA in neutral-alkaline arable soils amended with varying amounts of NH_4^+ has been sparsely documented. Multiple AOA lineages including *Nitrosopumilales-η* (Shi *et al*., 2016), *Nitrosopumilales-*γ (Verhamme *et al.*, 2011), *Nitrososphaerales-α*-3.2.1 (Xia *et al.*, 2011; Shi *et al.*, 2016), and *Nitrosocosmicus* lineage (Wang *et al.*, 2015; Pan *et al.*, 2018) have been found to proliferate in these soil ecosystems, especially for the last one which could grow under NH_3 concentrations preferred by copiotrophic AOB (Jung *et al.*, 2016; Lehtovirta-Morley *et al.*, 2016; Sauder *et al.*, 2017). However, in all soils tested here, OTUs of *Nitrosocosmicus* lineage were in low abundance and not affected by any treatments, and phylotypes responding to treatments were restricted to *Nitrososphaerales*. Moreover, when released from competition with AOB, AOA OTUs stimulated by the addition of high urea concentrations were taxonomically constrained, with all belonging to *Nitrososphaerales-α*-3.2.1 and *α*-3.2.4 lineages. Phylogenetically, OTUs of *Nitrososphaerales-α*-3.2.4 lineage were closely related to *N. gargensis*, while those of *Nitrososphaerales-α*-3.2.1 were associated with *N. viennensis* EN76, *Nitrososphaera* sp. JG1, and *N. evergladensis* SR1. These strains grew optimally under pHs ranging from 6.5 to 7.5 (Tourna *et al.*, 2011; Kim *et al.*, 2012; Zhalnina *et al.*, 2014), and phylotypes closely related to them have been classified as being alkalinophilic (Gubry-Rangin *et al.*, 2011; Oton *et al.*, 2016). Besides, when directly assessed in environmental studies including those using stable isotopic probing analysis, phylotypes within these lineages grew to a moderate extent in microcosms that were regularly spiked with NH_4^+ at a concentration of 100 μg NH_4^+-N g^{-1} soil (Xia *et al.*, 2011; Wang *et al.*, 2015; Shi *et al.*, 2016; Pan *et al.*, 2018). Thus, it appears that AOA affiliating to *Nitrososphaerales-α*-3.2.1 and *α*-3.2.4 lineages adapt to growth in NH_4^+-rich alkaline soils. Notwithstanding, their rapid growth under such high NH_4^+ concentrations adopted here (i.e. 200 μg NH_4^+-N g^{-1} soil) was still unexpected, as the reported inhibitory concentrations of NH_3 for these taxa are much lower than the theoretical values in Urea+1-Octyne treatment, especially for Urea+DMPP treatments (the highest value of 356 μM NH_3 for EN76 *vs*. lowest concentration of 2375 μM in Urea+DMPP treatments) (Tourna *et al.*, 2011; Kim

et al., 2012). Thus, it is likely that these phylotypes occupy a much broader niche than previously described, and they are highly susceptible to the competition from their bacterial counterpart.

On the other hand, the promotion of growth of AOA in Urea+1-Octyne treatment might be associated with mixotrophic activities, since not all AOA are obligate chemolithoautotrophs (Spang *et al.*, 2012; Zhalnina *et al.*, 2014; Kerou *et al.*, 2016; Vuillemin *et al.*, 2019), and some of them could be promoted by the addition of low-molecular-weight organic compound (Mußmann *et al.*, 2011; Tourna *et al.*, 2011). To exclude this possibility, DMPP, a nitrification inhibitor with distinctive heterocyclic chemical structure, was additionally adopted to inhibit the growth of AOB based on earlier findings (Shi *et al.*, 2016; Fan *et al.*, 2019). Our results suggested that the amendment of soils with 1-octyne or DMPP led to the enrichment of the same AOA phylotypes both within and across each soil tested, thus proving that the acceleration of AOA growth in Urea+1-Octyne and Urea+DMPP treatments was indeed attributed to their chemolithotrophy. However, unexpectedly, 1-octyne was far less effective at reducing the growth of AOB than previously reported (Taylor *et al.*, 2013; Hink *et al.*, 2018). Some AOB OTUs increased in the Urea+1-Octyne treatment, particularly those related to *Nitrosospira multiformis* whose growth had been previously demonstrated to be abolished by a lower concentration of 1-octyne (Taylor *et al.*, 2013). It is less likely that this stems from restricted diffusion or leakage of 1-octyne in the experimental systems, given that low concentrations of C_2H_2 completely abolished the growth of both AOA and AOB. Regardless of mechanisms, the lower inhibition efficiency of 1-octyne did not compromise our conclusion. Rather, the inhibition gradient created by Urea, Urea+1-Octyne, and Urea+DMPP treatments provided a unique opportunity to disentangle the effect of interaction between AOA and AOB. Hereby, we were able to show that the growth of AOA was closely coupled with the magnitude to which the growth of AOB was inhibited, and DMPP is a more effective and specific inhibitor against AOB than 1-octyne in the soils examined.

Besides, the experimental design adopted here allowed us to explore the potential ecological coherence of major phylogenetic lineages. We found that, in addition to those enriched by the high-ammonium amendment, the majority of changed OTUs within the same lineage showed a similar response pattern to a given treatment across soils. For instance, our results confirmed that the neutral-alkalinophilic *Nitrososphaerales-δ* lineage dominated the AOA assemblage in all soils tested (Gubry-Rangin *et al.*, 2011; Oton *et al.*, 2016), but most of OTUs therein were insensitive to amendment with urea or inhibitors across soils. Currently, no cultured representative has been identified in this lineage, therefore its ecological function in the soil is still unknown (Alves *et al.*, 2018). In contrast, changed OTUs in *β*-1, *γ*-1.1, and *γ*-2.1 lineages were generally reduced by Urea+1-Octyne and Urea+DMPP treatments. In particular, those of *γ*-1.1 and *γ*-2.1 lineages were exceptionally enriched in Urea+C_2H_2 treatment of all soils tested, presumably implying a mixotrophic lifestyle of these lineages. Similarly, one earlier report documented that the addition of 10 Pa C_2H_2 failed to inhibit the growth of AOA in an alkaline arable soil (Jia and Conrad, 2009). Intriguingly, despite being closely related to *α*-3.2.4, OTUs of *Nitrososphaerales α*-3.2.3 lineage were inhibited by Urea but not by Urea+DMPP and Urea+1-Octyne treatments, this concurred with the finding that phylogenetically closely related AOA could show contrasting metabolic traits (Alves *et al.*, 2018). Overall, our results confirm that AOA are functionally heterogeneous (Alves *et al*., 2018), but the coherence of response pattern of phylotypes within the same lineage to a given treatment implies their similar ecophysiology.

Finally, our results reaffirmed that AOB of *Nitrosospira* cluster 3a dominated the nitrification activity in the ammonium-rich alkaline soils (Jia and Conrad, 2009; Xia *et al.*, 2011; Ouyang *et al.*, 2016), whereas the growth of AOA in Urea and Urea+1-Octyne treatments implies that they assume a considerable role in contributing to overall nitrification in these soils as well. Although our experimental design did not allow for an absolute partitioning of their relative contribution, the nearly linear buildup of NO_3^- and occurrence of only AOA growth in DMPP treatment across the soils enabled back-of-the-envelope estimates to be calculated. Assuming that each AOA strain contains two *amoA* gene copies (Spang *et al.*, 2012) and all AOA growth is due to autotrophic nitrification activity, the specific AOA nitrification rates estimated ranged from 1.06 to 2.48 fmol $cell^{-1}$ d^{-1}. This was very similar to that of *Nitrososphaera sp.* JG1 (1.4 fmol $cell^{-1}$ d^{-1}) (Kim *et al.*, 2012), and *Nitrosarchaeum koreense* MY1 (2.5 fmol $cell^{-1}$ d^{-1}) (Jung *et al.*, 2011), but much lower than that of EN76 strain (62.6 fmol $copy^{-1}$ d^{-1}) (Stieglmeier *et al.*, 2014); and Candidatus *Nitrosocosmicus franklandus* C13 (13.92 fmol $cell^{-1}$ d^{-1}) (Lehtovirta-Morley *et al.*, 2016). Consequently, it is estimated that AOA accounted for 2%, 9%, and 10% nitrification activities in Urea treatments of the Shihezi, Tianshui, and Luoyang soils, respectively. These matched the estimates reported by Xia *et al.* (2011) (1.51%--23.4%) and were marginally lower than measurements by Ouyang *et al*. (2016) (11.55%--16.77%). However, the partial inhibition of AOB by 1-octyne further increased AOA contribution ranging from 17% to 30%. Collectively, these results point to an important role for AOA in nitrification in NH_4^+-rich alkaline arable soils.

CONCLUSIONS

Our results revealed that if released from the competition by AOB, taxonomically constrained AOA phylotypes would prevail under NH_4^+-rich alkaline arable soils. The representative strains of these phylotypes have been previously believed to be sensitive to high NH_3 concentrations adopted here. Moreover, 1-octyne and DMPP treatment of urea-enriched soils supported identical AOA lineages, highlighting that growth acceleration of these AOA under high NH_3 conditions was attributed to chemolithotrophy. Overall, these findings support the viewpoint that direct competition for the substrate drives the niche differentiation between these AOA phylotypes and AOB in ammonium-rich alkaline soils, thus providing an alternative explanation for this phenomenon and further expanding our understanding of microbial nitrification and N cycling.

ACKNOWLEDGEMENTS

We thank Zhengqi Yang at the Tianshui Institute of Agricultural Sciences and Zhiqiang Li at the Shihezi Institute of Agricultural Sciences for soil sampling. This work was jointly supported by the grants from the National Key Research and Development Program of China (Nos. 2017YFD0200707 and 2017YFD0200102) and the Fundamental Research Funds for the Central Universities (No. 2019FZJD007) for Yongchao Liang, as well as National Natural Science Foundation of China (Approved No. 31800418) for Chang Yin. We are also grateful to the two anonymous reviewers for their instructive comments and suggestions.

REFERENCES

Alves R J E, Minh B Q, Urich T, von Haeseler A, Schleper C. 2018. Unifying the global phylogeny and environmental distribution of ammonia-oxidising archaea based on *amoA* genes. *Nat Commun.* **9**: 1517.

Chen S, Zhou Y, Chen Y, Gu J. 2018. fastp: an ultra-fast all-in-one FASTQ preprocessor. *Bioinformatics*. **34**: i884-i890.

Di H J, Cameron K C, Shen J P, Winefield C S, O'Callaghan M, Bowatte S, He J Z. 2009. Nitrification driven by bacteria and not archaea in nitrogen-rich grassland soils. *Nat Geosci.* **2**: 621-624.

Edgar R C, Haas B J, Clemente J C, Quince C, Knight R. 2011. UCHIME improves sensitivity and speed of chimera detection. *Bioinformatics*. **27**: 2194-2200.

Edgar R C. 2013. UPARSE: highly accurate OTU sequences from microbial amplicon reads. *Nat Methods*. **10**: 996-998.

Fan X, Yin C, Chen H, Ye M, Zhao Y, Li T, Wakelin S A, Liang Y. 2019. The efficacy of 3, 4-dimethylpyrazole phosphate on N_2O emissions is linked to niche differentiation of ammonia oxidizing archaea and bacteria across four arable soils. *Soil Biol Biochem.* **130**: 82-93.

Francis C A, Roberts K J, Beman J M, Santoro A E, Oakley B B. 2005. Ubiquity and diversity of ammonia-oxidizing archaea in water columns and sediments of the ocean. *Proc Natl Acad Sci USA.* **102**: 14683-14688.

Gubry-Rangin C, Hai B, Quince C, Engel M, Thomson B C, James P, Schloter M, Griffiths R I, Prosser J I, Nicol G W. 2011. Niche specialization of terrestrial archaeal ammonia oxidizers. *Proc Natl Acad Sci USA.* **108**: 21206.

Hatzenpichler R. 2012. Diversity, physiology, and niche differentiation of ammonia-oxidizing archaea. *Appl Environ Microbiol.* **78**: 7501-7510.

He J Z, Hu H W, Zhang L M. 2012. Current insights into the autotrophic thaumarchaeal ammonia oxidation in acidic soils. *Soil Biol Biochem.* **55**: 146-154.

Hink L, Gubry-Rangin C, Nicol G W, Prosser J I. 2018. The consequences of niche and physiological differentiation of archaeal and bacterial ammonia oxidisers for nitrous oxide emissions. *ISME J.* **12**: 1084-1093.

Hink L, Lycus P, Gubry-Rangin C, Frostegård Å, Nicol G W, Prosser J I, Bakken L R. 2017. Kinetics of NH_3-oxidation, NO-turnover, N_2O-production and electron flow during oxygen depletion in model bacterial and archaeal ammonia oxidisers. *Environ Microbiol.* **19**: 4882-4896.

Jia Z, Conrad R. 2009. Bacteria rather than Archaea dominate microbial ammonia oxidation in an agricultural soil. *Environ Microbiol.* **11**: 1658-1671.

Jones C M, Hallin S. 2019. Geospatial variation in co-occurrence networks of nitrifying microbial guilds. *Mol Ecol.* **28**: 293-306.

Jung M Y, Park S J, Min D, Kim J S, Rijpstra W I C, Sinninghe Damsté J S, Kim G-J, Madsen E L, Rhee S-K. 2011. Enrichment and characterization of an autotrophic ammonia-oxidizing archaeon of mesophilic Crenarchaeal Group I.1a from an agricultural soil. *Appl Environ Microbiol.* **77**: 8635.

Jung M Y, Kim J G, Sinninghe Damsté J S, Rijpstra W I C, Madsen E L, Kim S J, Hong H, Si O J, Kerou M, Schleper C. 2016. A hydrophobic ammonia-oxidizing archaeon of the *Nitrosocosmicus* clade isolated from coal tar-contaminated sediment. *Environ Microbiol Rep.* **8**: 983-992.

Kerou M, Offre P, Valledor L, Abby S S, Melcher M, Nagler M, Weckwerth W, Schleper C. 2016. Proteomics and comparative genomics of *Nitrososphaera viennensis* reveal the core genome and adaptations of archaeal ammonia oxidizers. *Proc Natl Acad Sci USA.* **113**: E7937-E7946.

Kim J G, Jung M Y, Park S J, Rijpstra W I, Sinninghe Damsté J S, Madsen E L, Min D, Kim J S, Kim G J, Rhee S K. 2012. Cultivation of a highly enriched ammonia-oxidizing archaeon of thaumarchaeotal group I.1b from an agricultural soil. *Environ Microbiol.* **14**: 1528-1543.

Kits K D, Sedlacek C J, Lebedeva E V, Han P, Bulaev A, Pjevac P, Daebeler A, Romano S, Albertsen M, Stein L Y. 2017. Kinetic analysis of a complete nitrifier reveals an oligotrophic lifestyle. *Nature.* **549**: 269.

Kits K D, Sedlacek C J, Lebedeva E V, Han P, Bulaev A, Pjevac P, Daebeler A, Romano S, Albertsen M, Stein L Y, Daims H, Wagner M. 2017. Kinetic analysis of a complete nitrifier reveals an oligotrophic lifestyle. *Nature.* **549**: 269-272.

Lehtovirta-Morley L E, Ross J, Hink L, Weber E B, Gubry-Rangin C, Thion C, Prosser J I, Nicol G W. 2016. Isolation of 'Candidatus *Nitrosocosmicus franklandus*', a novel ureolytic soil archaeal ammonia oxidiser with tolerance to high ammonia concentration. *FEMS Microbiol Ecol.* **92**: fiw057-fiw057.

Lehtovirta-Morley L E, Stoecker K, Vilcinskas A, Prosser J I, Nicol G W. 2011. Cultivation of an obligate acidophilic ammonia oxidizer from a nitrifying acid soil. *Proc Natl Acad Sci USA.* **108**: 15892-15897.

Leininger S, Urich T, Schloter M, Schwark L, Qi J, Nicol G W, Prosser J I, Schuster S C, Schleper C. 2006. Archaea predominate among ammonia-oxidizing prokaryotes in soils. *Nature.* **442**: 806-809.

Letunic I, Bork P. 2016. Interactive tree of life (iTOL) v3: an online tool for the display and annotation of phylogenetic and other trees. *Nucleic Acids Res.* **44**: W242-W245.

Magoč T, Salzberg S L. 2011. FLASH: fast length adjustment of short reads to improve genome assemblies. *Bioinformatics*. **27**: 2957-2963.

Martens-Habbena W, Berube P M, Urakawa H, de la Torre J R, Stahl D A. 2009. Ammonia oxidation kinetics determine niche separation of nitrifying Archaea and Bacteria. *Nature.* **461**: 976-979.

Mußmann, Marc, Brito I, Pitcher A, Sinninghe Damsté J S, Hatzenpichler R, Richter A, Nielsen J L, Nielsen P H, Müller A, Daims H, Wagner M, Head I M. 2011. Thaumarchaeotes abundant in refinery nitrifying sludges express *amoA* but are not obligate autotrophic ammonia oxidizers. *Proc Natl Acad Sci USA.* **108**: 16771-16776.

Offre P, Prosser J I, Nicol G W. 2009. Growth of ammonia-oxidizing archaea in soil microcosms is inhibited by acetylene. *FEMS Microbiol Ecol.* **70**: 99-108.

Oksanen J, Guillaume B, Friendly M, Kindt R, Legendre P, McGlinn D, Minchin P, O'Hara R. 2019. vegan: Community ecology package. R package version 2.5-6. https://CRAN.R-project.org/package=vegan. .

Oton E V, Quince C, Nicol G W, Prosser J I, Gubry-Rangin C. 2016. Phylogenetic congruence and ecological coherence in terrestrial Thaumarchaeota. *ISME J.* **10**: 85-96.

Ouyang Y, Norton J M, Stark J M, Reeve J R, Habteselassie M Y. 2016. Ammonia-oxidizing bacteria are more responsive than archaea to nitrogen source in an agricultural soil. *Soil Biol Biochem.* **96**: 4-15.

Pan H, Xie K, Zhang Q, Jia Z, Xu J, Di H, Li Y. 2018. Archaea and bacteria respectively dominate nitrification in lightly and heavily grazed soil in a grassland system. *Biol Fertil Soils.* **54**: 41-54.

Prosser J I, Nicol G W. 2012. Archaeal and bacterial ammonia-oxidisers in soil: the quest for niche specialisation and differentiation. *Trends Microbiol.* **20**: 523-531.

R Core team. 2019. R: A language and environment for statistical computing. Vienna, Austria. URL https://www.R-project.org/.

Rognes T, Flouri T, Nichols B, Quince C, Mahé F. 2016. VSEARCH: a versatile open source tool for metagenomics. *PeerJ*. **4**: e2584.

Sauder L A, Albertsen M, Engel K, Schwarz J, Nielsen P H, Wagner M, Neufeld J D. 2017. Cultivation and characterization of Candidatus *Nitrosocosmicus exaquare*, an ammonia-oxidizing archaeon from a municipal wastewater treatment system. *ISME J.* **11**: 1142-1157.

Shi X, Hu H W, Müller C, He J Z, Chen D, Suter H C. 2016. Effects of the nitrification Inhibitor 3,4-dimethylpyrazole phosphate on nitrification and nitrifiers in two contrasting agricultural soils. *Appl Environ Microbiol.* **82**: 5236-5248.

Spang A, Poehlein A, Offre P, Zumbragel S, Haider S, Rychlik N, Nowka B, Schmeisser C, Lebedeva E V, Rattei T, Bohm C, Schmid M, Galushko A, Hatzenpichler R, Weinmaier T, Daniel R, Schleper C, Spieck E, Streit W, Wagner M. 2012. The genome of the ammonia-oxidizing Candidatus *Nitrososphaera gargensis*: insights into metabolic versatility and environmental adaptations. *Environ Microbiol.* **14**: 3122-3145.

Stahl D A, de la Torre J R. 2012. Physiology and diversity of ammonia-oxidizing archaea. *Annu Rev Microbiol.* **66**: 83-101.

Stieglmeier M, Mooshammer M, Kitzler B, Wanek W, Zechmeister-Boltenstern S, Richter A, Schleper C. 2014. Aerobic nitrous oxide production through N-nitrosating hybrid formation in ammonia-oxidizing archaea. *ISME J.* **8**: 1135-1146.

Tamura K, Stecher G, Peterson D, Filipski A, Kumar S. 2013. MEGA6: Molecular Evolutionary Genetics Analysis Version 6.0. *Mol Biol Evol.* **30**: 2725-2729.

Tao R, Wakelin S A, Liang Y, Chu G. 2017. Response of ammonia-oxidizing archaea and bacteria in calcareous soil to mineral and organic fertilizer application and their relative contribution to nitrification. *Soil Biol Biochem.* **114**: 20-30.

Taylor A E, Vajrala N, Giguere A T, Gitelman A I, Arp D J, Myrold D D, Sayavedra-Soto L, Bottomley P J. 2013. Use of aliphatic n-alkynes to discriminate soil nitrification activities of ammonia-oxidizing Thaumarchaea and bacteria. *Appl Environ Microbiol.* **79**: 6544-6551.

Tourna M, Stieglmeier M, Spang A, Könneke M, Schintlmeister A, Urich T, Engel M, Schloter M, Wagner M, Richter A. 2011. *Nitrososphaera viennensis*, an ammonia oxidizing archaeon from soil. *Proc Natl Acad Sci USA.* **108**: 8420-8425.

Trivedi C, Reich P B, Maestre F T, Hu H-W, Singh B K, Delgado-Baquerizo M. 2019. Plant-driven niche differentiation of ammonia-oxidizing bacteria and archaea in global drylands. *ISME J.* **13**: 2727-2736.

Verhamme D T, Prosser J I, Nicol G W. 2011. Ammonia concentration determines differential growth of ammonia-oxidising archaea and bacteria in soil microcosms. *ISME J.* **5**: 1067-1071.

Vuillemin A, Wankel S D, Coskun Ö K, Magritsch T, Vargas S, Estes E R, Spivack A J, Smith D C, Pockalny R, Murray R W, D'Hondt S, Orsi W D. 2019. Archaea dominate oxic subseafloor communities over multimillion-year time scales. *Sci Adv.* **5**: eaaw4108.

Wang B, Zhao J, Guo Z, Ma J, Xu H, Jia Z. 2015. Differential contributions of ammonia oxidizers and nitrite oxidizers to nitrification in four paddy soils. *ISME J.* **9**: 1062-1075.

Xia W, Zhang C, Zeng X, Feng Y, Weng J, Lin X, Zhu J, Xiong Z, Xu J, Cai Z, Jia Z. 2011. Autotrophic growth of nitrifying community in an agricultural soil. *ISME J.* **5**: 1226-1236.

Yin C, Fan F, Song A, Fan X, Ding H, Ran W, Qiu H, Liang Y. 2017. The response patterns of community traits of N_2O emission-related functional guilds to temperature across different arable soils under inorganic fertilization. *Soil Biol Biochem.* **108**: 65-77.

Zhalnina K V, Dias R, Leonard M T, Dorr de Quadros P, Camargo F A O, Drew J C, Farmerie W G, Daroub S H, Triplett E W. 2014. Genome sequence of Candidatus *Nitrososphaera evergladensis* from Group I.1b enriched from everglades soil reveals novel genomic features of the ammonia-oxidizing archaea. *PloS one.* **9**: e101648.

Zhao J, Bello M O, Meng Y, Prosser J I, Gubry-Rangin C. 2020. Selective inhibition of ammonia oxidising archaea by simvastatin stimulates growth of ammonia oxidising bacteria. *Soil Biol Biochem.* **141**: 107673.

Figure captions

Fig. 1 The dynamics of ammonium (a, b, and c) and nitrate (d, e, and f) in Luoyang (a, d), Shihezi (b, e) and Tianshui (c, f). Means ± 1SE (n = 3) were shown. Urea was supplemented in all treatments except CK at days 6, 12, 18, and 24 to reach the targeted ammonium concentration (*i.e.*, 200 μg N g^{-1} dry soil), the times at which urea was supplemented were labeled with arrows.

Fig. 2 The changes in abundances of AOA (a, b, and c) and AOB (d, e, and f) in Luoyang (a, d), Shihezi (b, e) and Tianshui (c, f) soil during incubation. Means ± 1SE (n = 3) were shown.

Fig. 3 NMDS analysis of the community composition of AOA (a-c) and AOB (d-f) for Luoyang (a, d), Shihezi (b, d), and Tianshui (c, f). All OTUs whose relative abundances were significantly changed by treatments were shown as circles (*i.e.*, the colored numbers). Their relative abundances were log-scaled with the diameter of circles, and phylogenetic affiliations were mapped to different colors. NS, *Nitrososphaerales*.

Fig. 4 The composition of AOA OTUs that were significantly different among treatments within soils. The unrooted phylogenetic tree was shown on the left of the heatmap. The cluster analysis result of samples based on the Bray-Curtis dissimilarity matrix was shown above the heatmap. For clarity, only OTUs with relative abundance higher than 0.1% across all samples were shown.

Fig. 1

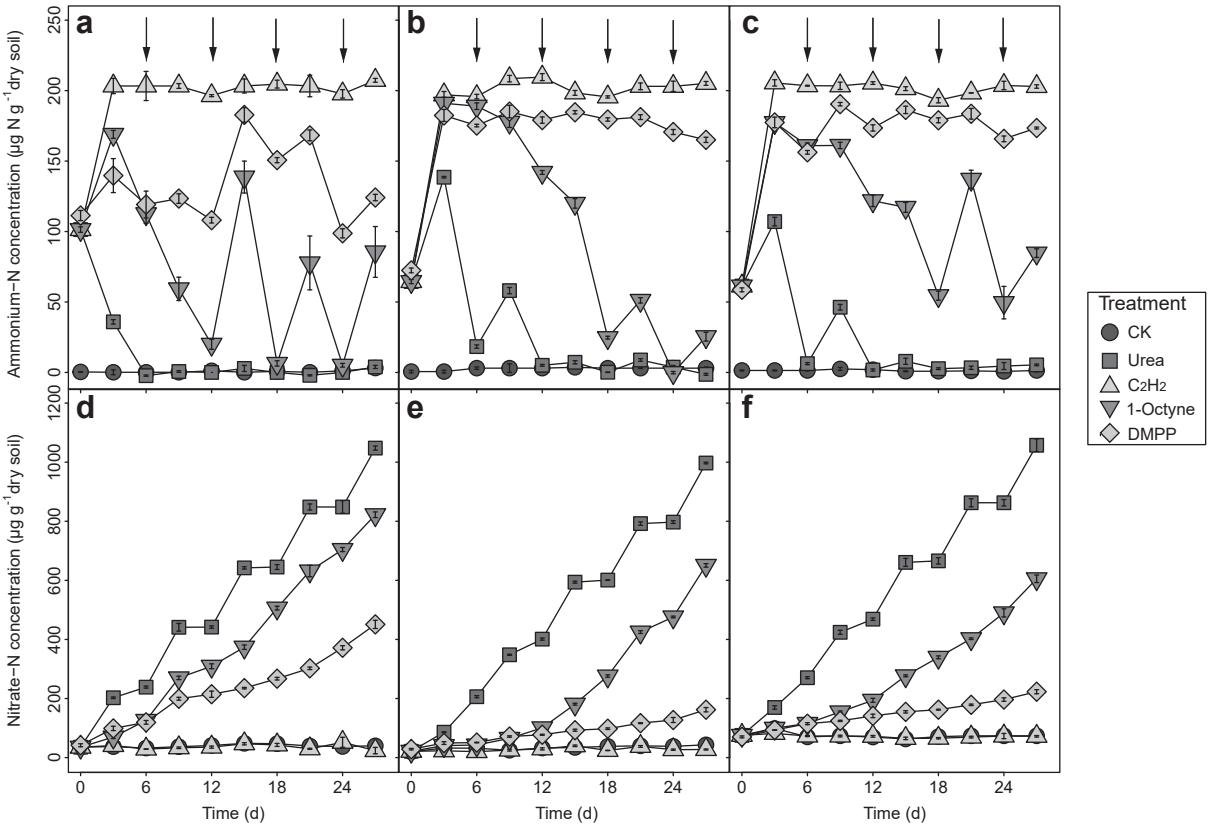
a
b
c
d
e
f
Ammonium−N concentration (μg N g−1dry soil)
Nitrate−N concentration (μg g−1dry soil)
Time (d)
Treatment
CK
Urea
C2H2
1-Octyne
DMPP

Fig. 2

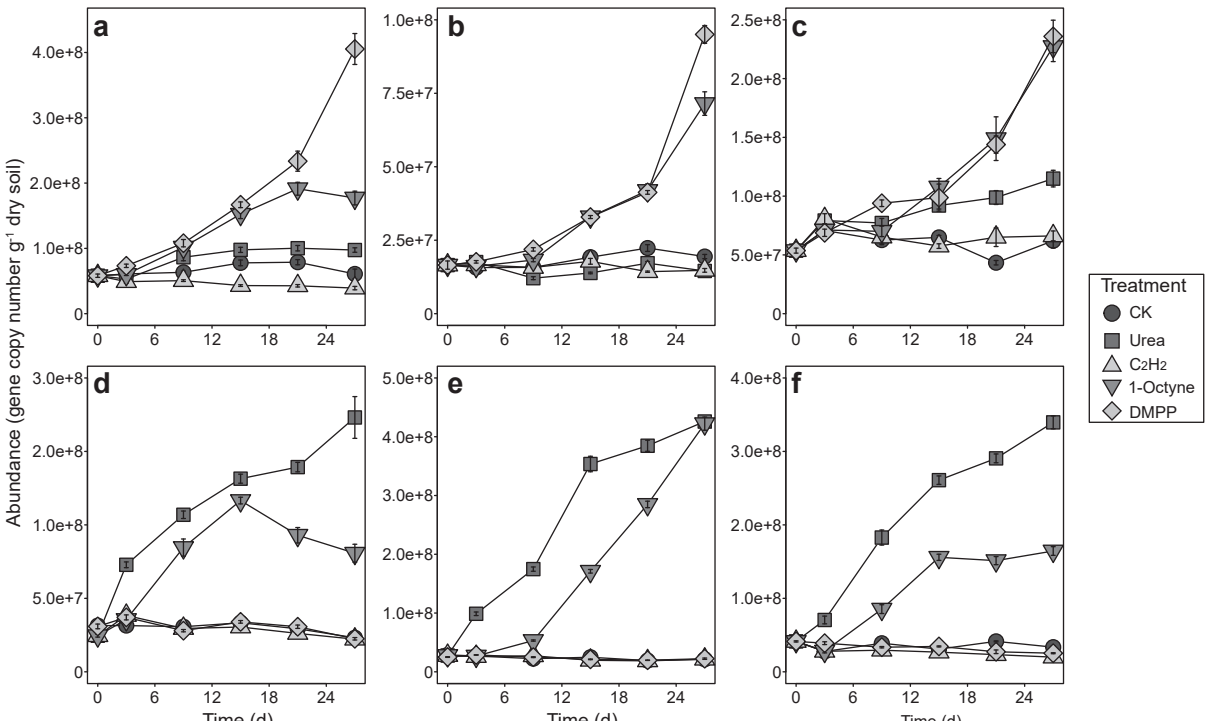
a
b
c
d
e
f
Abundance (gene copy number g-1 dry soil)
Time (d)
Treatment
CK
Urea
C2H2
1-Octyne
DMPP

Fig. 4

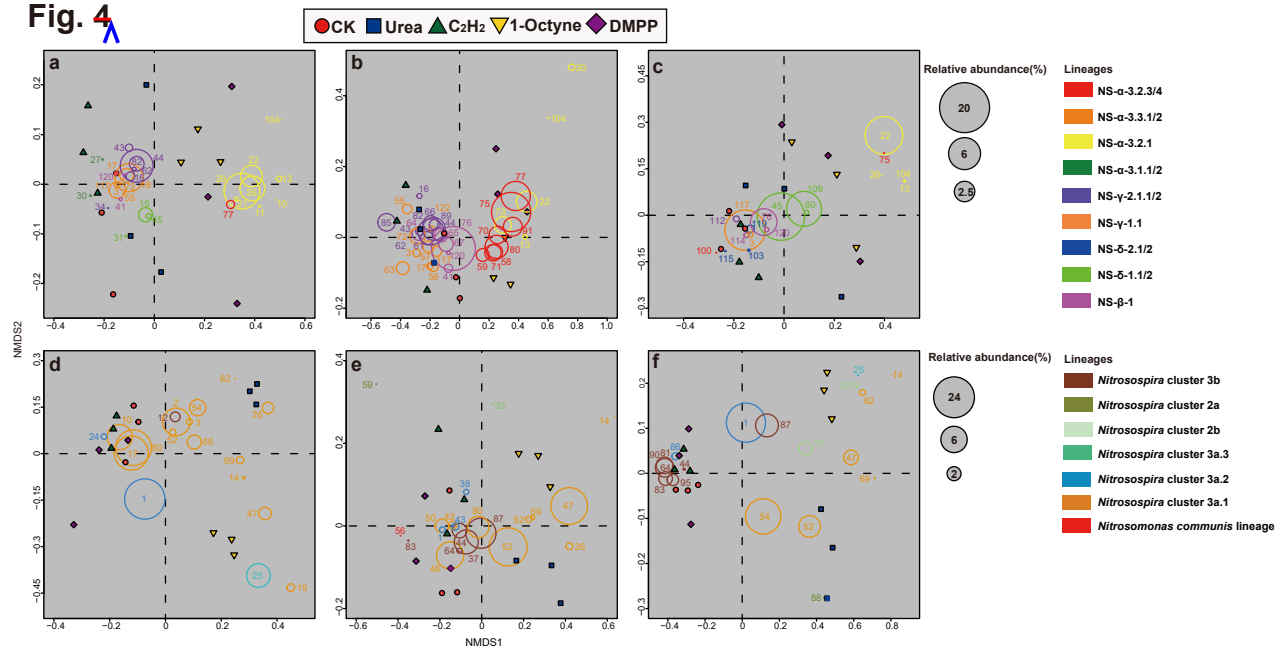
CK
Urea
C2H2
1-Octyne
DMPP
a
b
c
d
e
f
NMDS1
NMDS2
Relative abundance(%)
20
6
2.5
Lineages
NS-α-3.2.3/4
NS-α-3.3.1/2
NS-α-3.2.1
NS-α-3.1.1/2
NS-γ-2.1.1/2
NS-γ-1.1
NS-δ-2.1/2
NS-δ-1.1/2
NS-β-1
Relative abundance(%)
24
6
2
Lineages
Nitrosospira cluster 3b
Nitrosospira cluster 2a
Nitrosospira cluster 2b
Nitrosospira cluster 3a.3
Nitrosospira cluster 3a.2
Nitrosospira cluster 3a.1
Nitrosomonas communis lineage

Fig. 5

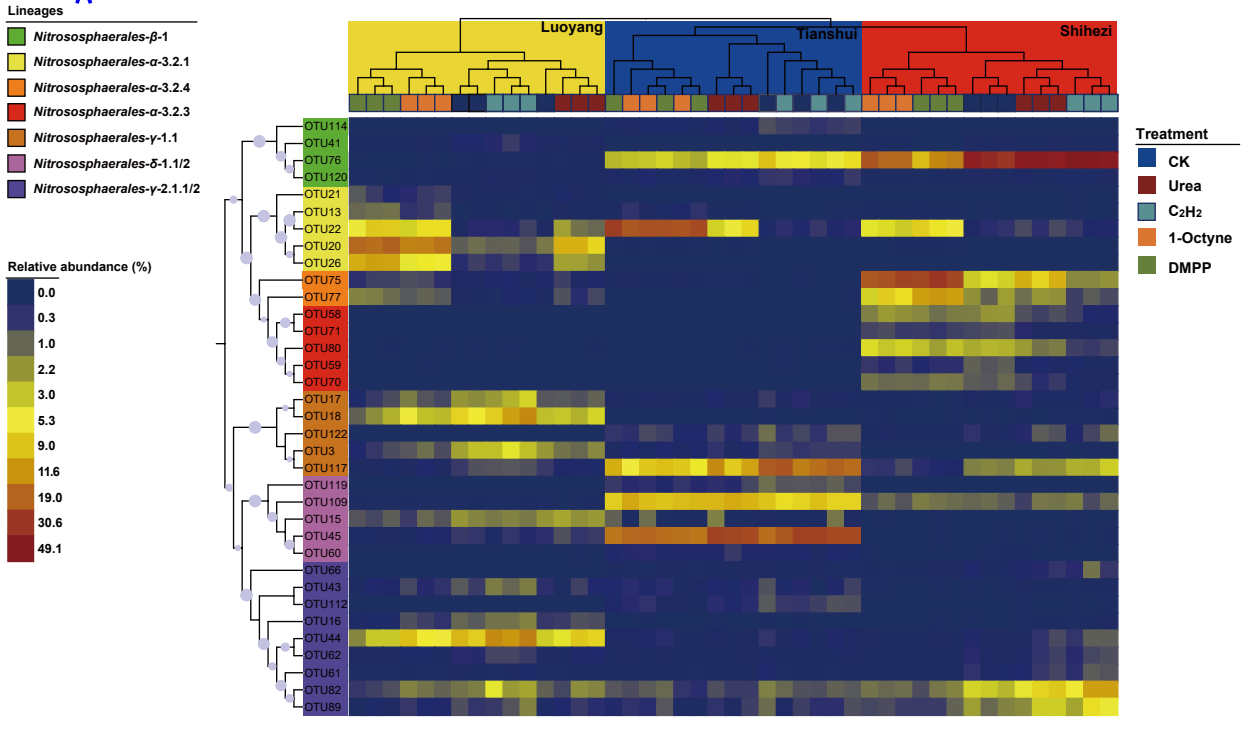
Lineages
Nitrososphaerales-β-1
Nitrososphaerales-α-3.2.1
Nitrososphaerales-α-3.2.4
Nitrososphaerales-α-3.2.3
Nitrososphaerales-γ-1.1
Nitrososphaerales-δ-1.1/2
Nitrososphaerales-γ-2.1.1/2
Relative abundance (%)
0.0
0.3
1.0
2.2
3.0
5.3
9.0
11.6
19.0
30.6
49.1
Luoyang
Tianshui
Shihezi
OTU114
OTU41
OTU76
OTU120
OTU21
OTU13
OTU22
OTU20
OTU26
OTU75
OTU77
OTU58
OTU71
OTU80
OTU59
OTU70
OTU17
OTU18
OTU122
OTU3
OTU117
OTU119
OTU109
OTU15
OTU45
OTU60
OTU66
OTU43
OTU112
OTU16
OTU44
OTU62
OTU61
OTU82
OTU89
Treatment
CK
Urea
C2H2
1-Octyne
DMPP